

# Effects of neutrino temperatures and mass hierarchies on the detection of supernova neutrinos

Shao-Hsuan Chiu\* and T. K. Kuo†

*Department of Physics, Purdue University, West Lafayette, IN 47907*

## Abstract

Possible outcomes of neutrino events at both Super-Kamiokande and SNO for a type-II supernova are analyzed considering the uncertainties in SN neutrino spectra (temperature) at emission, which may complicate the interpretation of the observed events. With the input of parameters deduced from the current solar and atmospheric experiments, consequences of direct-mass hierarchy  $m_{\nu_\tau} \gg m_{\nu_\mu} > m_{\nu_e}$  and inverted-mass hierarchy  $m_{\nu_e} > m_{\nu_\mu} \gg m_{\nu_\tau}$  are investigated. Even if the  $\nu$  temperatures are not precisely known, we found that future experiments are likely to be able to separate the currently accepted solutions to the solar neutrino problem (SNP): large angle MSW, small angle MSW, and the vacuum oscillation, as well as to distinguish between the direct and inverted mass hierarchies of the neutrinos.

Typeset using REVTeX

---

\*chiu@physics.purdue.edu

†tkkuo@physics.purdue.edu

## I. INTRODUCTION

During the past few decades, elaborate solar neutrino [1] and atmospheric neutrino [2] experiments have provided a wealth of convincing evidences for the existence of massive neutrinos and neutrino mixing, which could have an essential impact on particle physics, astrophysics and cosmology. Attentions have been focused on solving the puzzles of unexpected discrepancies between calculated and observed neutrino fluxes. Instead of the more difficult and unlikely solution from an improved solar model [3], the solar  $\nu_e$  deficit could be reconciled with the prediction if neutrino oscillations occur either in vacuum or in the presence of solar matter.

The flavor oscillation can be parameterized by the mass-squared differences of the neutrino mass eigenstates  $\Delta m^2 \equiv m_i^2 - m_j^2$  ( $i, j = 1, 2, 3$ ) and  $\theta_{ij}$ , the mixing angles between weak eigenstates and mass eigenstates of the neutrinos ( $\theta_{ij} \leq \frac{\pi}{4}$  is assumed). In terms of these parameters, the just-so vacuum oscillation [4] requires  $6 \times 10^{-11} \leq \Delta m^2 \leq 60 \times 10^{-11}$  eV<sup>2</sup> and  $\sin^2 2\theta \simeq 1$ , while the MSW resonant effect [5] in the Sun becomes important if  $4 \times 10^{-6}$  eV<sup>2</sup>  $\leq \Delta m^2 \leq 7 \times 10^{-5}$  eV<sup>2</sup>,  $\sin^2 2\theta \simeq 0.6 - 0.9$  (large angle solution), or  $3 \times 10^{-6}$  eV<sup>2</sup>  $\leq \Delta m^2 \leq 12 \times 10^{-6}$  eV<sup>2</sup>,  $0.003 \leq \sin^2 2\theta \leq 0.01$  (small angle solution) [6]. Recent atmospheric neutrino data from the Super-Kamiokande [7] further provide a strong evidence in support of neutrino oscillation as the cause to deficit of muon neutrinos, provided  $\Delta m^2 \sim 10^{-2} - 10^{-3}$  eV<sup>2</sup> and  $\sin^2 2\theta > 0.82$ . It is clear that this solution to the neutrino anomaly in the atmosphere represents quite a distinct area in the parameter space as compared to that of the solar neutrino deficit. Based on the conclusive LEP experiment at CERN [8] that there are three flavors of light, active neutrinos participating in the weak interaction, a direct-mass hierarchy  $m_{\nu_\tau} \gg m_{\nu_\mu} > m_{\nu_e}$ , with  $\Delta_{32}^2 \simeq \Delta_{31}^2 \gg \delta_{21}^2$  ( $\Delta_{32}^2 \equiv m_3^2 - m_2^2$  and  $\delta_{21}^2 \equiv m_2^2 - m_1^2$ ) naturally accommodates the scales of both the two mass-squared differences and provides solutions to both puzzles: the conversion  $\nu_e \rightarrow \nu_\mu$  causes the observed deficit in the solar  $\nu_e$  flux and the vacuum oscillation  $\nu_\mu \rightarrow \nu_\tau$  suppresses the  $\nu_\mu$  flux in the atmosphere.

In addition to the Sun and the atmosphere, type-II supernovae are also natural sources that emit neutrinos. Despite the first-ever observation of SN neutrino signals from SN 1987A [9], detailed neutrino spectral shapes have not yet been determined with certainty due to low statistics and the physical processes that are not well understood. This difficulty is accompanied by, for instance, the uncertainties in the characteristic temperatures  $T_\nu$  as neutrinos were emitted from the neutrino-spheres. Consequently, the interpretation of future measurements of SN neutrinos would contain ambiguity in that the observed spectrum, which may have been deformed through conversion processes, could be simulated by different set of parameters at different temperatures.

It is therefore worthwhile to investigate how the uncertainty in  $T_\nu$  could impact the interpretation of events at terrestrial detectors. In this paper, the parameters that solve solar and atmospheric neutrino problems are taken as inputs, a natural choice as also adopted by some earlier works [10] [11]. In addition, with the uncertainty in  $T_\nu$  considered, we study whether a particular set of parameters could be singled out by future observations of SN neutrinos.

Unlike solar neutrinos, the initial neutrino flux from a supernova contains all flavors of neutrino:  $\nu_e, \nu_\mu, \nu_\tau$  and their anti-particles. Under the direct-mass hierarchy of neutrinos,

the original  $\nu$  spectra will be modified by the MSW effect as neutrinos propagate through the resonance. The  $\bar{\nu}$  spectra, on the contrary, is subject only to vacuum oscillation which yields an large averaged survival probability of  $\bar{\nu}_e : P(\bar{\nu}_e \rightarrow \bar{\nu}_e) \geq \frac{1}{2}$ . The high-energy  $\bar{\nu}_\mu(\bar{\nu}_\tau)$  would not be converted to the easily detectable  $\bar{\nu}_e$  (for instance, at Super-Kamiokande) through the MSW effect unless neutrino masses are inverted, in which case the heavier mass eigenstate has a larger component in  $\nu_e$  than in  $\nu_\mu$  or  $\nu_\tau$ . Since the mixing angles are defined in the first octant, the weak eigenstates  $\nu_\tau, \nu_\mu$ , and  $\nu_e$  are predominant in the mass eigenstates  $\nu_3, \nu_2$ , and  $\nu_1$ , respectively. Under the direct-mass hierarchy where  $m_{\nu_\tau} > m_{\nu_\mu} > m_{\nu_e}$ , the mass eigenstates follow the hierarchy  $m_3 > m_2 > m_1$ , while in the inverted-mass hierarchy, for instance,  $m_{\nu_e} > m_{\nu_\mu} > m_{\nu_\tau}$ , the pattern  $m_1 > m_2 > m_3$  follows. Some models and phenomenological consequences involving inverted neutrino masses have been discussed [12]. Although current MSW solutions to the solar neutrino problem (SNP) have excluded  $\nu_e$  as the heavier eigenstate, the inverse hierarchy could remain viable if the just-so vacuum oscillation is the solution for the SNP. If the inverted masses do apply and the resonance conditions for the anti-neutrinos are met, this could lead to an effective conversion between  $\bar{\nu}_e$  and the higher-energy  $\bar{\nu}_\mu(\bar{\nu}_\tau)$  to yield copious  $\bar{\nu}_e$ -type events in the earth-bound detector. With the uncertainty in  $T_\nu$  considered, it is our second goal to investigate influences of both the direct and inverted mass hierarchies to future observations of SN neutrinos and how future measurements can play a role in this unsettled issue of direct versus inverted neutrino masses.

This paper is organized as follows. In section II we summarize the general features of stellar collapse and properties of the emitted neutrinos, and show how the uncertainty in neutrino temperature could affect the outcomes in the detector. Section III and Section IV contain more general results expected from the future observations at both Super-Kamiokande and SNO, for direct and inverted masses, respectively. Based on the measurements, possible schemes which could provide discrimination among input parameters and between the two mass hierarchies are proposed. Section V contains discussions and our concluding remarks.

## II. DETECTION OF SUPERNOVA NEUTRINOS

### A. SN neutrinos and neutrino parameters

A massive star ( $M \geq 8M_\odot$ ) becomes unstable at the last stage of its evolution. When the mass of the iron core reaches the Chandrasekhar limits ( $\sim 1.4M_\odot$ ), it begins to collapse into a compact object of extremely high density, and the gravitational binding energy is released in the form of neutrinos. Mayle *et al.* [13] have pointed out that the total emitted energy, the averaged neutrino luminosity, and the mean neutrino energy are independent of the explosive mechanism but depend only on the mass of the initial iron core. Regardless of the details of collapsed and bounce, it is well established that to form a typical neutron star after the collapse, an amount of  $\sim 3 \times 10^{53}$  erg, about 99% of the binding energy would be released in the form of neutrinos. Each (anti)neutrino species will carry away about the same amount of energy.

Neutrinos are emitted from a collapsed star through two different processes: neutronization burst during the pre-bounce phase and thermal emission in the post-bounce phase. The neutronization burst of a  $\nu_e$  flux is produced by the electron capture on protons:

$e^- + p \rightarrow n + \nu_e$ . The thermal emission creates  $\nu\bar{\nu}$  pairs of all three flavors via the annihilation of  $e^+e^-$  pairs:  $e^+e^- \rightarrow \nu_\ell + \bar{\nu}_\ell$  ( $\ell = e, \mu, \tau$ ). The duration of neutronization burst lasts about a few millisecond and takes away 1%-10% of the total binding energy. The thermal emission phase has a much wider spread of time structure, in the order of 10 seconds.

The initial neutrino spectrum is usually approximated by a Fermi-Dirac or a Boltzmann distribution with a constant temperature and zero chemical potential. To reduce the high-energy tail of the Fermi-Dirac distribution, some elaborate models introduce a nonzero chemical potential [14]. It is clear that the event numbers in a detector depend crucially on the  $\nu$  temperature. However, the numerical calculations based upon various models and physical arguments give rise to relatively wide ranges of temperature for each neutrino species [15] and this uncertainty in  $T_\nu$  could complicate the signatures concerning the oscillation of neutrinos from a supernova.

One may refer to Ref. [16] for a review of neutrino oscillations. Although all the three flavors are emitted from a supernova, the phenomenon of SN neutrino oscillation can be well described through  $P(\nu_e \rightarrow \nu_e)$  and  $P(\bar{\nu}_e \rightarrow \bar{\nu}_e)$  [17]. Under the direct-mass hierarchy, the probability  $P(\bar{\nu}_e \rightarrow \bar{\nu}_e)$  is nearly independent of energy and is approximated by the vacuum oscillation expression. The probability  $P(\nu_e \rightarrow \nu_e)$  is energy-dependent and contains four parameters under a proper parameterization of the mixing matrix in the full 3- $\nu$  formalism:  $\delta_{21}^2, \Delta_{32}^2 \simeq \Delta_{31}^2, \theta_{21}, \phi_{31}$ . In what follows, these four parameters will simply be denoted as  $\delta^2, \Delta^2, \theta$ , and  $\phi$ , respectively.

Among the above four parameters, the angle  $\phi$  is special in certain aspect. In addition to the limit  $\phi < 12^\circ$  at 90% C.L. set by the CHOOZ [19] long baseline reactor in the disappearance mode  $\bar{\nu}_e \rightarrow \bar{\nu}_x$ , an analysis in Ref. [6] also has given allowed ranges of  $\delta^2$  and  $\sin^2 2\theta$  for  $\phi < 20^\circ$ . Note that to zeroth order of  $\delta^2/\Delta^2$ , the probability becomes [18]

$$P(\nu_e \rightarrow \nu_e) \simeq \cos^4 \phi P_{2\nu} + \sin^4 \phi. \quad (2.1)$$

One may examine  $\phi$  in more details through the iso-probability contours for SN neutrinos at several distinct scales of  $\delta^2/E_\nu$ , as shown in Figure 1. Within the interested range of  $\theta$ , ( $\sin^2 2\theta \geq 0.003$ , or  $\log_{10} \tan^2 2\theta \geq -2.5$ ), the  $P(\nu_e \rightarrow \nu_e)$  contours are almost independent of  $\phi$  for  $\phi < 12^\circ$  ( $\log_{10} \tan^2 2\phi < -0.7$ ). The parameter  $\phi$  begins to show slight influence on  $P(\nu_e \rightarrow \nu_e)$  contours only at very small  $\theta$  and very large  $\phi$ . Hence, for our purpose the choice of  $\phi$  within  $\phi < 20^\circ$  would only affect the results slightly. The value  $\phi = 10^\circ$  will be adopted for definiteness. As for other input parameters, the following are taken:

Large angle MSW solution(LA):  $\delta^2 = 10^{-5} \text{ eV}^2, \sin^2 2\theta = 0.75$ .

Small angle MSW solution(SA):  $\delta^2 = 6 \times 10^{-6} \text{ eV}^2, \sin^2 2\theta = 0.0075$ .

Just-so vacuum solution(JS):  $\delta^2 = 3 \times 10^{-10} \text{ eV}^2, \sin^2 2\theta \simeq 1$ .

## B. The Complication In Observed Events

In what follows, an initial flux described by a Fermi-Dirac spectrum with zero chemical potential will be assumed. The detailed time evolution during the cooling phase has been ignored, while the averaged magnitudes and effective temperatures of  $\nu(\bar{\nu})$  flux are used instead [20]. The event numbers at the detectors  $\nu$  for the neutrino of type  $\ell$  are estimated by

$$N_\ell = \frac{Z L_\ell}{4\pi D^2} \int dE_\nu n_\ell(E_\nu, T_\ell) \sigma_\ell(E_\nu) P_\ell(E_\nu). \quad (2.2)$$

Here  $Z$  is the number of targets in the detector,  $L_\ell$  is the initial number of  $\nu_\ell$ ,  $D$  is the distance between the supernova and the earth,  $\sigma_\ell(E_\nu)$  is the cross section for the corresponding reaction,  $P_\ell(E_\nu)$  is the surviving probability for  $\nu_\ell$ ,  $T_\ell$  is the temperature for  $\nu_\ell$ , and

$$n_\ell(E_\nu, T_\ell) \simeq 0.5546 \frac{E_\nu^2}{T_\ell^3 [1 + \exp(\frac{E_\nu}{T_\ell})]}. \quad (2.3)$$

In evaluating the surviving probability, the electron number per nucleon is assumed to remain a constant ( $Y_e \approx 0.42$ ) and the density profile outside the neutrino-sphere ( $r \geq 10^7$  cm) is described by the power-law  $\rho \sim r^{-3}$ .

To grasp the picture on how uncertainties in neutrino temperatures could affect the interpretation of observed events, we may tentatively assume  $T_{\nu_e} = 3$  MeV,  $T_{\nu_x} = T_{\bar{\nu}_x} = 6$  MeV ( $x = \mu, \tau$ ), and compare outcomes from  $T_{\bar{\nu}_e} = 3$  MeV and  $T_{\bar{\nu}_e} = 4.5$  MeV. At Super-Kamiokande [21], contributions from the inverse beta decay  $\bar{\nu}_e + p \rightarrow e^+ + n$  predominate due to the high cross section. Events from other interactions:  $\nu_\ell(\bar{\nu}_\ell) + e^-$ , ( $\ell = e, \mu, \tau$ ) [22] and  $\nu_e(\bar{\nu}_e) + {}^{16}\text{O}$  [23], will also be included in our calculations although these events accumulate up to less than 5% of the  $\bar{\nu}_e + p$  events. The threshold energy is taken to be 5 MeV and the detector efficiency is assumed to be 100%. For 32 kton of water, one expects roughly  $\sim 10^4$  neutrino events for a type II supernova at the center of our galaxy ( $\sim 10$  kpc away).

Since the cross section for  $\bar{\nu}_e + p$  is proportional to  $E_\nu^2$ , and  $E_\nu \simeq 3.1T_\nu$  for the Fermi-Dirac distribution, a larger temperature gap between  $\bar{\nu}_e$  and  $\bar{\nu}_x$  would cause a more severely distorted spectra from the original one. Hence the difference between  $T_{\bar{\nu}_e}$  and  $T_{\bar{\nu}_x}$  determines to what extent the events are enhanced by oscillation.

For the direct masses where  $m_{\nu_\tau} \gg m_{\nu_\mu} > m_{\nu_e}$ , possible results of the ratio  $OSC/NO$  ( $OSC$  indicates oscillation, and  $NO$  indicates the case of no oscillation) using specific input parameters LA, SA, and JS are shown in Figure 2. The curves representing LA and SA are due to MSW effects of the  $\nu$ -type events and the vacuum oscillation of the  $\bar{\nu}$ -type events, while the JS curve is due to vacuum oscillations of both  $\nu$ - and  $\bar{\nu}$ -type events. One observes that JS parameters could raise event numbers most effectively, an increase of  $\sim 55\%$  is possible at  $T_{\bar{\nu}_e} \simeq 3$  MeV ( $\frac{T_{\bar{\nu}_e}}{T_{\bar{\nu}_x}} \simeq 0.5$ ). The enhancement decreases as  $T_{\bar{\nu}_e}$  approaches  $T_{\bar{\nu}_x}$ . Near a particular point where  $T_{\bar{\nu}_e} \simeq T_{\bar{\nu}_x}$ , the conversion of  $\bar{\nu}_e$  to  $\bar{\nu}_x$  would not alter the original  $\bar{\nu}_e$  spectrum, all the scenarios yield  $OSC/NO \simeq 1$  and are indistinguishable among each other.

The complication arises from the fact that if, for instance,  $OSC/NO = 1.3$  is observed, this observation is then either due to LA parameters at  $T_{\bar{\nu}_e} \simeq 3.6$  eV or the JS parameters at  $T_{\bar{\nu}_e} \simeq 4$  eV. The uncertainties in neutrino temperatures would therefore render a wide range of predictions at the detectors. Informations such as the clues for oscillation and neutrino parameters would be hard to understand or even lost due to this complication.

### III. GENERAL CONSEQUENCES FROM THE DIRECT MASSES

## A. Super-Kamiokande

For the observation of SN neutrinos, the extremely distinct time structures between the neutronization burst and the beginning of thermal emission would allow a clear separation at the  $H_2O$  Cherenkov detector. These two groups of events are discussed separately.

The spectral shape and the total energy of  $\nu_e$  from the early pre-bounce burst is still poorly known. For the purpose of qualitative discussion, the spectrum is arbitrarily chosen to be the same as that of thermal  $\nu_e$  (Fermi-Dirac) with the same mean energy and a total of 5% the binding energy of a typical neutron star ( $E_b$ ). During this early phase, one expects to observe the forward directional events due to elastic scattering  $\nu_e + e^-$  and the backward events from  $\nu_e + {}^{16}O$ . These neutronization events are summarized in Table I. We note that the forward events are relatively insensitive to the uncertainty in  $\nu_e$  temperature. The oscillation signature manifests itself through the drastically reduced forward events as compared to the original one, although practically the separation among LA, SA, and JS using events observed during this early phase is difficult.

The backward events on the other hand, are more sensitive to  $T_{\nu_e}$ . The difficulty associated with the backward events comes from the extremely small numbers. If  $T_{\nu_e} = 3$  MeV and the total neutrino energy at this stage is down to  $\sim 1\%$  of  $E_b$ , the backward events are practically unobservable. Because of the rapidly increased cross section for  $\nu_e + {}^{16}O$  at higher energy:  $\sigma \sim (E - E_{th})^2$ , the situation could be improved if  $T_{\nu_e}$  is higher or if the neutrinos emitted during this phase have larger energy partition, which is quite model-dependent. Unlike the backward events, the forward event numbers are roughly in the order of 10 even if  $T_{\nu_e} = 3$  MeV and the  $\nu_e$  flux takes away as low as  $\sim 1\%$  of  $E_b$ .

By using the numerous  $e^+$  emitted from the inverse beta decay, the distorted  $\bar{\nu}_e$  spectrum would be determined with better statistics. To account for the uncertainties in  $T_{\nu_e}$  and  $T_{\nu_x}$ , we may let  $T_{\nu_x} = \alpha T_{\bar{\nu}_e}$ ,  $T_{\nu_e} = \beta T_{\bar{\nu}_e}$  and compare the outcomes for  $T_{\bar{\nu}_e} = 4$  MeV, 5 MeV, and 6 MeV. The parameters  $\alpha$  and  $\beta$  are allowed to vary within  $1.4 \leq \alpha \leq 1.8$  and  $0.6 \leq \beta \leq 1$  to roughly include the temperature ranges given by current models. Expected ranges for the ratios  $R \equiv I/F$  are summarized in Table II, where  $I$  includes events from the inverse beta decay and the neutrino interactions with oxygen,  $F$  represents the forward scattering events. For  $T_{\bar{\nu}_e} = 4$  MeV, there are two overlapped areas in  $R$ : between NO, SA and between JS, LA. The same overlapping structure remains for  $T_{\bar{\nu}_e} = 5$  MeV and  $T_{\bar{\nu}_e} = 6$  MeV. Despite the wealthy information conveyed through the  $e^+$  spectrum at Super-Kamiokande, from Table II it seems unlikely that a clear separation among input parameters could be achieved using the otherwise model-independent quantity  $R$  unless the uncertainties in neutrino temperatures are reduced significantly.

## B. SNO

The neutral current(NC) breakup reactions of deuterium in SNO [24] are flavor-blind for neutrinos:

$$\nu_\ell + d \rightarrow n + p + \nu_\ell, (E_{th} = 2.22MeV) \quad (3.1)$$

$$\bar{\nu}_\ell + d \rightarrow n + p + \bar{\nu}_\ell, (E_{th} = 2.22MeV) \quad (3.2)$$

where  $\ell = e, \nu, \tau$ . The charged current reactions include two parts,

$$CC_1 : \nu_e + d \rightarrow p + p + e^-, (E_{th} = 1.44\text{MeV}) \quad (3.3)$$

$$CC_2 : \bar{\nu}_e + d \rightarrow n + n + e^+, (E_{th} = 4.03\text{MeV}). \quad (3.4)$$

With 1 kton of  $D_2O$  and a threshold energy  $\sim 5$  MeV ( 100% detection efficiency assumed), both  $CC_1$  and  $CC_2$  should roughly yield event numbers in the order of  $10^2$ . The ratios  $r_1 = \frac{NC}{CC_1}$  at SNO seem to provide a solution as to how a particular set of parameter could be singled out, as will be shown below.

One may arbitrarily fix  $T_{\nu_e}$  and parameterize other temperatures in a similar way: let  $T_{\nu_x} = \lambda T_{\nu_e}$  and allow an uncertainty in  $T_{\bar{\nu}_e}$  as well:  $T_{\bar{\nu}_e} = \eta T_{\nu_e}$ , with  $1.8 \leq \lambda \leq 2.6$  and  $1.1 \leq \eta \leq 1.7$ . The ratio  $r_1 = \frac{NC}{CC_1}$  for  $T_{\nu_e} = 3, 4$  and  $5$  MeV are listed in Table III. We found that even if the uncertainties in  $T_{\nu_x}$  and  $T_{\bar{\nu}_e}$  may complicate the interpretation of observed events, each of the candidates gives rise to a distinct region in  $\frac{NC}{CC_1}$ . In practical, if uncertainties in  $\lambda$  and  $\eta$  can be reduced in the future, it would enable a smaller spread in each  $r_1$  for a better separation.

## IV. CONSEQUENCES FROM THE INVERTED MASSES

### A. Vacuum oscillation versus MSW effect

In the light of MSW effect, distinctions between direct and inverted masses would most likely appear in the observed neutrino spectra. If the just-so vacuum oscillation is favored over the MSW oscillations as solution to the SNP, both direct ( $m_{\nu_\tau} \gg m_{\nu_\mu} > m_{\nu_e}$ ) and inverted-mass schemes ( $m_{\nu_e} > m_{\nu_\mu} \gg m_{\nu_\tau}$ ) are allowed since  $\nu_e$  flux can also be converted to  $\nu_x$  through the vacuum oscillation if neutrino masses are inverted. The  $\bar{\nu}_e$  flux on the contrary, would go through the MSW resonance if the mass hierarchy is inverted. This conversion would presumably enlarge the  $\bar{\nu}_e$ -type event rates effectively at Super-Kamiokande. Without conflicting current solar and atmospheric neutrino data, we would focus on the JS parameters:  $-\delta^2 \sim 10^{-10}\text{eV}^2$  and large  $\theta$ , for a further investigation under the inverted mass scheme  $m_{\nu_e} > m_{\nu_\mu} \gg m_{\nu_\tau}$ .

The possible SN  $\bar{\nu}_e$  spectra are shown in Figure 3. Curve *A* is the original  $\bar{\nu}_e$  spectrum and curve *B* represents the distorted one through the just-so vacuum oscillation under the direct-mass scheme while curve *C* is obtained from the MSW conversion under the inverted-mass scheme. Curves *B* and *C* nearly overlap, implying that the matter effect is not as prominent as expected, and that the MSW effect under the inverted-mass hierarchy is almost identical to the vacuum oscillation under the direct-mass hierarchy for  $\bar{\nu}_e$  at this particular region of parameter space. Furthermore, the extremely small observable difference at the detectors would make the identification between the two mass patterns very difficult. The reason becomes clear if the required conditions for a MSW resonance and an adiabatic transition to occur are both considered [25]: A density profile  $\rho \sim r^{-3}$  would yield  $|\delta^2| \sim 10^{-8} - 10^5 \text{eV}^2$  relevant to the MSW oscillation in the supernova. This mass scale is much larger than the mass scale of JS parameters ( $|\delta^2| \sim 10^{-10} \text{eV}^2$ ). Therefore a very effective conversion of  $\bar{\nu}_e$  to  $\bar{\nu}_x$  in a supernova is unlikely for either direct or inverted masses if the JS parameters

are applied. The strong conversion of  $\bar{\nu}_e$  to  $\bar{\nu}_x$  is actually disfavored by some analyses based on the SN 1987A data [26]. If either LA or SA MSW conversion is favored over the just-so vacuum oscillation, the case for the inverted hierarchy  $m_{\nu_e} > m_{\nu_\mu} \gg m_{\nu_\tau}$  would then become shaky or can even be ruled out.

## B. Super-Kamiokande and SNO

An alternative approach might shed some clues to the inverted-mass scheme and its outcomes. We may characterize consequences for the oscillation  $\bar{\nu}_e \leftrightarrow \bar{\nu}_x$  by the surviving probability of  $\bar{\nu}_e$  in three limit cases:  $P(\bar{\nu}_e \rightarrow \bar{\nu}_e) \sim 1$ ,  $P(\bar{\nu}_e \rightarrow \bar{\nu}_e) \sim \frac{1}{2}$ , and  $P(\bar{\nu}_e \rightarrow \bar{\nu}_e) \ll 1$ . The case  $P(\bar{\nu}_e \rightarrow \bar{\nu}_e) \sim 1$  indicates that no conversion occurs among  $\bar{\nu}_e$  and  $\bar{\nu}_x$ , which is equivalent to the outcome of having massless neutrinos, and the mass pattern would then unlikely be the main issue. The JS parameters, as already discussed, yield  $P(\bar{\nu}_e \rightarrow \bar{\nu}_e) \sim \frac{1}{2}$  for the MSW conversion (or equivalently, the vacuum oscillation under the direct-mass scheme). One is therefore motivated to further study the consequences for a complete conversion of  $\bar{\nu}_e$  flux to  $\bar{\nu}_x$ , where  $P(\bar{\nu}_e \rightarrow \bar{\nu}_e) \ll 1$ . As pointed out by Totani *et al.* [25], due to statistical uncertainties in experiments and the inconsistency among current analyses, one cannot completely exclude the possibility of full conversion. We may tentatively neglect details of the physical conditions and parameters that required for a complete conversion to occur, and assume that the probability  $P(\bar{\nu}_e \rightarrow \bar{\nu}_e)$  remains approximately a constant within interested range of the neutrino energy.

To reasonably account for the contributions from  $\nu_e$  and  $\nu_x$  fluxes to the total events when a complete conversion occurs in the anti-neutrinos sector, one may first consider the contours of  $OSC/NO$  for events from the inverse beta decay only. Under the inverted-mass scheme, a wide range of  $-\delta^2$  and  $\theta$  are shown in Figure 4. Given  $T_{\bar{\nu}_e} = 4.5$  MeV,  $T_{\nu_e} = 3$  MeV and  $T_{\nu_x} = T_{\bar{\nu}_x} = 6$  MeV, the JS parameters ( $|\delta^2| \sim 10^{-10}$  eV<sup>2</sup> and large  $\theta$ ) roughly result in a 20% increment to the event number. After a full conversion of the anti-neutrinos in which  $P(\bar{\nu}_e \rightarrow \bar{\nu}_e) \ll 1$ , one would expect to observe a sizable increase in the ratio  $OSC/NO$ . Therefore a larger  $|\delta^2|$  and a smaller  $\tan^2 2\theta$ , at least several orders of magnitude, are required for a full conversion to occur. The smallness of  $\theta$ , alone with the small  $\phi$ , fix the surviving probability of  $\nu_e$  very close to unity. Hence, a full conversion of  $\bar{\nu}_e$  to  $\bar{\nu}_x$  would be accompanied by nearly unchanged  $\nu_e$  and  $\nu_x$  fluxes:  $P(\nu_e \rightarrow \nu_e) \sim 1$ . The expected ratios  $R \equiv I/F$  at the Super-Kamiokande are listed in Table IV. Despite the better statistic provided by the  $\bar{\nu}_e$ -type events at Super-Kamiokande, the detection is however not unique to the  $\bar{\nu}_e$  flux, the uncertainties in  $T_{\nu_e}$  and  $T_{\nu_x}$  therefore make the separation between  $P(\bar{\nu}_e \rightarrow \bar{\nu}_e) \ll 1$  (complete conversion) and  $P(\bar{\nu}_e \rightarrow \bar{\nu}_e) \sim \frac{1}{2}$  difficult.

At the SNO detector, the charged-current channel  $\bar{\nu}_e + d \rightarrow n + n + e^+$  is unique to  $\bar{\nu}_e$ . This channel can be distinguished from the neutral-current events and the other charged-current channel induced by  $\nu_e$ . Therefore the measurement of  $\bar{\nu}_e + d$  events at SNO should be sensitive to the full conversion of  $\bar{\nu}_e$  to  $\bar{\nu}_x$ . Ratios of the neutral-current events to the charged-current events  $\bar{\nu}_e + d$ , denoted as  $\frac{NC}{CC_2}$ , are shown in Table V. We also present values of the same ratio under the direct-mass scheme in Table VI as a comparison.

We observe that for a particular  $T_{\nu_e}$ , both direct and inverted schemes yield a nearly identical range of  $\frac{NC}{CC_2}$  if the JS parameters are applied, this verifies a previous argument. The valuable message from this ratio is that for a particular  $T_{\nu_e}$ , a complete conversion of

the  $\bar{\nu}_e$  flux through MSW resonance represents a unique range of  $\frac{NC}{CC_2}$  as compared to other scenarios, including that of the direct masses.

Typical  $\frac{NC}{CC_2}$  contours for inverted masses are shown in Figure 5, where  $T_{\nu_e} = 3$  MeV,  $T_{\bar{\nu}_e} = 4.5$  MeV, and  $T_{\nu_x} = T_{\bar{\nu}_x} = 6$  MeV are assumed. Since the neutral-current reaction is blind to the oscillation, a complete swap of  $\bar{\nu}_e$  and  $\bar{\nu}_x$  fluxes would definitely yield smaller  $\frac{NC}{CC_2}$ . Calculations show that  $\frac{NC}{CC_2} \sim 2.95$  for a complete conversion and indicate that  $-\delta^2 > 10^{-2}$  eV<sup>2</sup> and  $\tan^2 2\theta < 10^{-2}$  are required for a near complete conversion to occur.

Tables V and VI suggest that for the detection of SN neutrinos, the direct and inverted masses could be distinguishable if a nearly complete conversion of  $\bar{\nu}_e$  to  $\bar{\nu}_x$  occurs, which yields a low  $\frac{NC}{CC_2}$  and signals the existence of inverted-mass pattern. Since the MSW effects become important for supernova neutrinos at  $10^{-8} < \Delta m^2 < 10^5$  eV<sup>2</sup>, a future supernova would provide a test ground for  $-\delta^2 > 10^{-2}$  eV<sup>2</sup>. If the nearly full conversion  $\bar{\nu}_e \leftrightarrow \bar{\nu}_x$  is observed in the SN neutrino flux, the consequences may have certain implications in that the required parameter spaces for a full conversion are obviously disfavored by current solar neutrino data, while the future solar and atmospheric observations may not severely change the mass scales required to explain the solar and the atmospheric neutrino deficits.

## V. DISCUSSIONS AND CONCLUSIONS

Under the constraints of mass scale from solar and atmospheric neutrinos, the  $3 - \nu$  scenario naturally leads to four possible hierarchies (one direct and three inverted): (1)  $m_{\nu_\tau} \gg m_{\nu_\mu} > m_{\nu_e}$ , (2)  $m_{\nu_\mu} > m_{\nu_e} \gg m_{\nu_\tau}$ , (3)  $m_{\nu_e} > m_{\nu_\mu} \gg m_{\nu_\tau}$ , (4)  $m_{\nu_\tau} \gg m_{\nu_e} > m_{\nu_\mu}$ . Case 1 is the normal, direct mass scheme. For Case 2,  $|\delta^2|$  in the mass scale of the MSW solution has been discussed [11]. In our analysis we have applied Case 3, in which the mass scale of  $|\delta^2|$  is suitable for the vacuum solution of SNP ( $10^{-10}$  eV<sup>2</sup>). Case 3 and Case 2 become equivalent if  $|\delta^2| \sim 10^{-10}$  eV<sup>2</sup> since the MSW and the vacuum oscillations for the  $\bar{\nu}_e$  flux would be nearly identical at this mass scale, as shown in Section IV. For Case 4 to survive,  $|\delta^2|$  needs to be in the order of  $10^{-10}$  eV<sup>2</sup> for the vacuum solution to apply. Therefore, consequences for Case 4 and Case 1 become equivalent in the detection of supernova neutrinos if  $|\delta^2| \sim 10^{-10}$  eV<sup>2</sup>.

In this work, responses at both Super-Kamiokande and SNO detectors to neutrino fluxes coming from a supernova are studied under the consideration of uncertainties in neutrino temperatures. In particular, some phenomenological consequences for direct-mass and inverted-mass patterns of neutrinos are compared. We may summarize our results as follows. (a) Uncertainties in neutrino temperatures can allow various interpretations of neutrino parameters. We have shown this through the expected outcomes at Super-Kamiokande for SN neutrinos. (b) The three candidates LA, SA, and JS manifest differently in the ratio  $\frac{NC}{CC_1}$  at SNO even if the uncertainties in neutrino temperature are allowed. Future detection of SN neutrinos at SNO would be able to single out favored mass and mixing parameters from the three candidates. (c) In addition to the direct-mass pattern, the inverted-mass scenario  $m_{\nu_e} > m_{\nu_\mu} \gg m_{\nu_\tau}$  is investigated since it can allow the vacuum solution to the solar neutrino problem. By using the event ratio  $\frac{NC}{CC_2}$  in SNO, the direct-mass ( $m_{\nu_\tau} \gg m_{\nu_\mu} > m_{\nu_e}$ ) and the inverted-mass ( $m_{\nu_e} > m_{\nu_\mu} \gg m_{\nu_\tau}$ ) could be distinguished if a nearly complete  $\bar{\nu}_e \leftrightarrow \bar{\nu}_x$  conversion occurs in the anti-neutrino section.

## ACKNOWLEDGMENTS

S.C. would like to thank Nien-Po Chen and Sadek Mansour for suggestions in preparing the manuscript. T. K. is supported in part by the DOE, Grant no. DE-FG02-91ER40681.

## REFERENCES

- [1] R. Davis Jr., Prog. in Nucl. and Part. Phys. **32** (1994); SAGE Collaboration, J. N. Abdurashitov *et al.*, Phys. Lett. B **328**, 234 (1994); GALLEX Collaboration, P. Anselmann *et al.*, Phys. Lett. B **357**, 237 (1995); KamioKande Collaboration, K. Hirata *et al.*, Phys. Rev. D **44**, 2241 (1991).
- [2] KamioKande Collaboration, Phys. Lett. B **335**, 237 (1994); IMB Collaboration, Phys. Rev. Lett. **66**, 2561 (1989); Soudan 2 Collaboration, Nucl. Phys. B **38**, 337 (1995) (Proc. Suppl.).
- [3] J. N. Bahcall and M. H. Pinsonneault, Rev. Mod. Phys. **64**, 885 (1992).
- [4] S. L. Glashow, P. J. Kernan, and L. M. Krauss, Phys. Lett. B **445**, 412 (1999).
- [5] L. Wolfenstein, Phys. Rev. D **17**, 2369 (1978); S. P. Mikheyev and A. Yu. Smirnov, Yad. Fiz. **42**, 1441 (1985) [ Sov. J. Nucl. Phys. **42**, 913 (1986)].
- [6] T. Sakai, O. Inagaki, and T. Teshima, Int. J. Mod. Phys. A **14**, 1953 (1999).
- [7] Super-Kamiokande Collaboration, Phys. Rev. Lett. **81**, 1562 (1998).
- [8] Particle Data Group, Phys. Rev. D **54**, 1 (1996).
- [9] K. Hirata *et al.*, Phys. Rev. Lett. **58**, 1490 (1987); R. M. Bionta *et al.*, Phys. Rev. Lett. **58**, 1494 (1987).
- [10] Gautam Dutta, D. Indumathi, M. V. N. Murthy and G. Rajasekaran, hep-ph/9907372 (1999).
- [11] A. S. Dighe and A. Yu. Smirnov, hep-ph/9907423 (1999).
- [12] G. G. Raffelt and J. Silk, Phys. Lett. B **366**, 429 (1996); D. O. Caldwell and R. N. Mohapatra, Phys. Lett. B **354**, 371 (1995); G. M. Fuller, J. R. Primack and Y. -Z. Qian, Phys. Rev. D **52**, 1288 (1995).
- [13] R. Mayle, J. R. Wilson, and D. Schramm, Astrophys. J. **318**, 288 (1987).
- [14] B. Jegerlehner, F. Neubig, and G. Raffelt, Phys. Rev. D **54**, 2784 (1996); T. Totani, K. Sato, H. Dalhed, and J. R. Wilson, Astrophys. J. **496**, 216 (1998).
- [15] D. Schramm, Comments Nucl. Part. Phys. (1987); A. Burrows, D. Klein, and R. Gandhi, Phys. Rev. D **45**, 3361 (1992); J. F. Beacom and P. Vogel, Phys. Rev. D **58**, 053010 (1998), and references therein.
- [16] T. K. Kuo and J. Pantaleone, Rev. Mod. Phys. **61**, 937 (1989).
- [17] T. K. Kuo and J. Pantaleone Phys. Rev. D **37**, 298 (1988).
- [18] G. L. Fogli, E. Lisi, and D. Montanino, Phys. Rev. D **54**, 2048 (1996).
- [19] M. Apollonio *et al.*, CHOOZ Collaboration, Phys. Lett. B **420**, 397 (1998).
- [20] E. Kh. Akhmedov and Z. G. Berezhiani, Nucl. Phys. B **373**, 479 (1992).
- [21] Super-Kamiokande Collaboration, Phys. Lett. B **433**, 9 (1998).
- [22] J. Arafune and M. Fukugita, Phys. Rev. Lett. **59**, 367 (1987).
- [23] W. Haxton, Phys. Rev. D **36**, 2283 (1987).
- [24] M. E. Moorhead, in *Neutrino Astrophysics*, ed. M. Altmann *et al.* (Ringberg, Germany, 1997).
- [25] T. Totani and K. Sato, Int. J. Mod. Phys. D **5**, 519 (1996).
- [26] A. Yu. Smirnov, D. N. Spergel, and J. N. Bahcall, Phys. Rev. D **49**, 1389 (1994); B. Jegerlehner, F. Neubig, and G. Raffelt, Phys. Rev. D **54**, 1194 (1996).

TABLES

	$T_{\nu_e} = 3$ MeV		$T_{\nu_e} = 4$ MeV		$T_{\nu_e} = 5$ MeV	
	backward	forward	backward	forward	backward	forward
NO	7	68	20	71	38	72
LA	2	26	5	27	10	29
SA	5	41	14	46	28	49
JS	3	38	9	39	19	42

TABLE I. Total expected backward and forward events at Super-Kamiokande for the neutronization burst of neutrinos from a typical supernova  $\sim 10$  kpc away.

	$T_{\bar{\nu}_e} = 4$ MeV	$T_{\bar{\nu}_e} = 5$ MeV	$T_{\bar{\nu}_e} = 6$ MeV
NO	15.9 - 16.9	20.0 - 20.9	23.9 - 25.0
LA	18.3 - 20.9	22.7 - 25.4	26.7 - 29.4
SA	16.4 - 18.1	20.9 - 23.4	24.8 - 27.7
JS	19.1 - 22.5	23.7 - 26.8	27.2 - 29.6

TABLE II. The ratio  $R \equiv I/F$  in Super-Kamiokande for thermally emitted neutrinos. Here the mass hierarchy is direct. The uncertainties in  $T_{\nu_e}$  and  $T_{\nu_x}(T_{\bar{\nu}_x})$  give rise to the spread in  $R$ .

	$T_{\nu_e} = 3$ MeV	$T_{\nu_e} = 4$ MeV	$T_{\nu_e} = 5$ MeV
NO	5.4 - 9.0	5.3 - 7.9	5.1 - 6.5
LA	2.6 - 2.8	2.7 - 2.9	2.7 - 2.9
SA	3.9 - 5.1	4.0 - 5.1	4.0 - 4.9
JS	3.1 - 3.5	3.2 - 3.5	3.2 - 3.5

TABLE III.  $r_1 = \frac{NC}{CC_1}$ , the ratios of neutral-current event numbers to charged-current event numbers ( $\nu_e + d \rightarrow p + p + e^-$ ) in SNO for thermally emitted neutrinos. Here the mass hierarchy is direct.

	$T_{\bar{\nu}_e} = 4$ MeV	$T_{\bar{\nu}_e} = 5$ MeV	$T_{\bar{\nu}_e} = 6$ MeV
JS(INVERTED)	19.3 - 22.8	23.6 - 26.5	27.3 - 29.6
COMPLETE	22.1 - 28.3	26.3 - 30.6	29.2 - 30.9

TABLE IV. The ratio  $R \equiv I/F$  at Super-Kamiokande under the inverted-mass scheme.

	$T_{\nu_e} = 3 \text{ MeV}$	$T_{\nu_e} = 4 \text{ MeV}$	$T_{\nu_e} = 5 \text{ MeV}$
JS	3.4 - 4.0	3.2 - 3.8	3.1 - 3.7
COMPLETE	2.6 - 3.2	2.6 - 3.1	2.6 - 3.0

TABLE V.  $\frac{NC}{CC_2}$ , the ratios of neutral-current event numbers to charged-current event numbers ( $\bar{\nu}_e + d \rightarrow n + n + e^+$ ) in SNO for thermally emitted neutrinos. Here neutrino masses are inverted. This table can be compared with Table VI where neutrino masses are direct. A complete conversion yields the lowest value of  $\frac{NC}{CC_2}$  for a given  $T_{\nu_e}$ .

	$T_{\nu_e} = 3 \text{ MeV}$	$T_{\nu_e} = 4 \text{ MeV}$	$T_{\nu_e} = 5 \text{ MeV}$
NO	3.5 - 11.4	3.4 - 8.8	3.2 - 6.8
LA	3.4 - 4.7	3.2 - 4.4	3.2 - 4.1
SA	3.5 - 9.4	3.3 - 7.7	3.2 - 6.2
JS	3.4 - 4.1	3.2 - 3.9	3.1 - 3.7

TABLE VI.  $\frac{NC}{CC_2}$  for the thermal emission of neutrinos in SNO, with direct masses.

## FIGURES

FIG. 1.  $P(\nu_e \rightarrow \nu_e)$  for SN neutrinos at (a)  $\delta^2/E = 10^{-5}$  eV<sup>2</sup>/MeV, (b)  $\delta^2/E = 10^{-7}$  eV<sup>2</sup>/MeV, (c)  $\delta^2/E = 10^{-9}$  eV<sup>2</sup>/MeV, and (d)  $\delta^2/E = 10^{-11}$  eV<sup>2</sup>/MeV. Here  $\delta^2$  is the mass-squared difference in eV<sup>2</sup> and  $E$  is neutrino energy in MeV.

FIG. 2. Predicted curves of the ratio  $OSC/NO$  in Super-Kamiokande for the direct masses. We have defined  $Y \equiv OSC/NO$ ,  $X \equiv \frac{T_{\bar{\nu}_e}}{T_{\bar{\nu}_x}}$ . Here  $T_{\nu_e} = 3$  MeV,  $T_{\bar{\nu}_x} = 6$  MeV are assumed, and  $T_{\bar{\nu}_e}$  are allowed to vary from 3 MeV to 6 MeV as indicated by  $X \equiv \frac{T_{\bar{\nu}_e}}{T_{\bar{\nu}_x}}$ .

FIG. 3. Expected  $\bar{\nu}_e$  spectra from a supernova. Curve  $A$  represents the original  $\bar{\nu}_e$  without any conversion; curve  $B$  is the one distorted by the vacuum oscillation under direct-mass hierarchy while  $C$  is the expected curve for  $\bar{\nu}_e$  after MSW conversion, with the same parameters applied in  $B$  but under inverted-mass scheme.  $B$  and  $C$  are nearly indistinguishable.

FIG. 4. The contour plot of  $OSC/NO$  from the events of inverse beta decay. The inverted masses are assumed. Here we have set  $T_{\bar{\nu}_e} = 4.5$  MeV,  $T_{\nu_e} = 3$  MeV and  $T_{\nu_x} = T_{\bar{\nu}_x} = 6$  MeV.

FIG. 5. Typical  $NC/CC_2$  contours in SNO under the inverted-mass scheme. Here  $T_{\nu_e} = 3$  MeV,  $T_{\bar{\nu}_e} = 4.5$  MeV and  $T_{\nu_x} = T_{\bar{\nu}_x} = 6$  MeV are assumed. A complete conversion of the  $\bar{\nu}_e$  flux to  $\bar{\nu}_x$  flux would yield  $NC/CC_2 \sim 2.95$ , which occurs at  $|\delta^2| > 10^{-2}$  eV<sup>2</sup>.

FIG. 1(a)

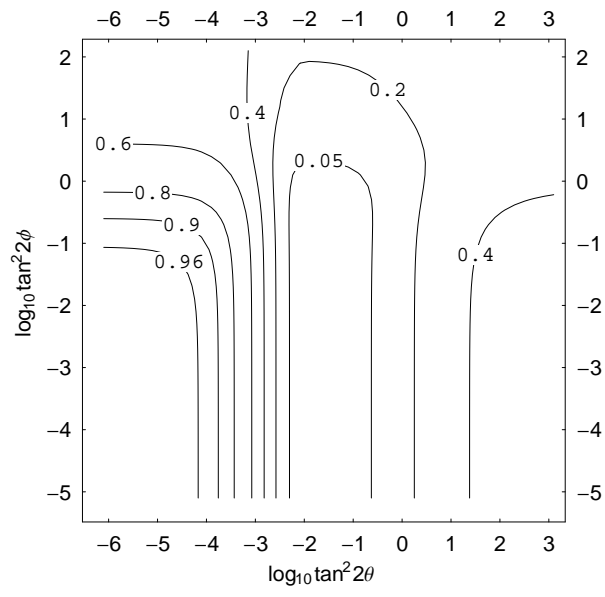


FIG. 1(b)

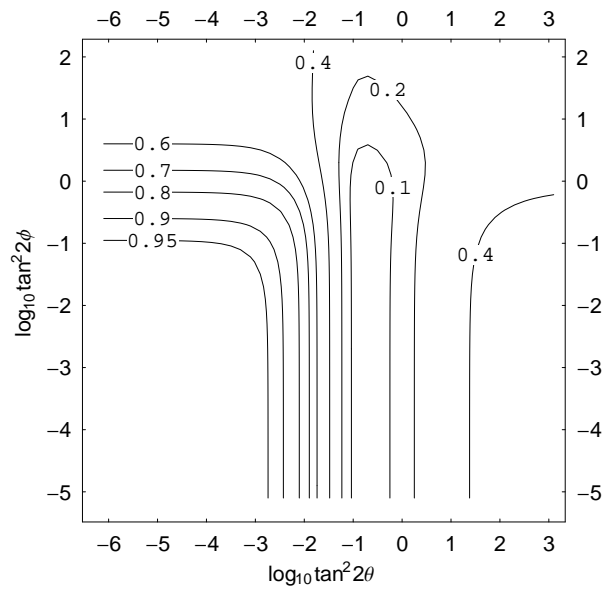


FIG. 1(c)

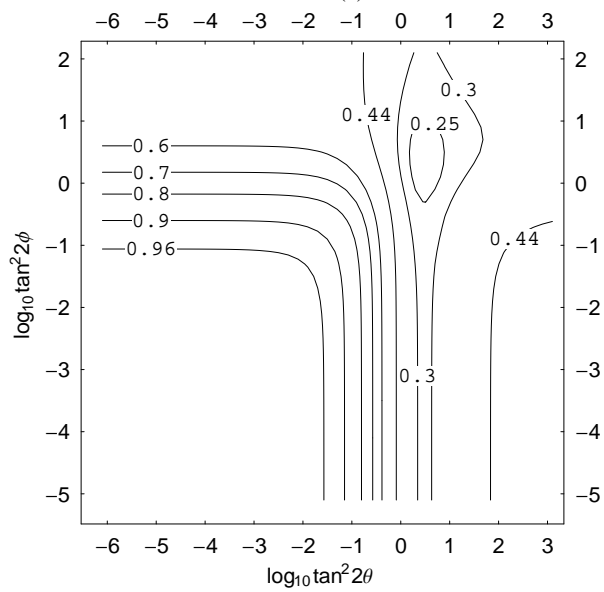


FIG. 1(d)

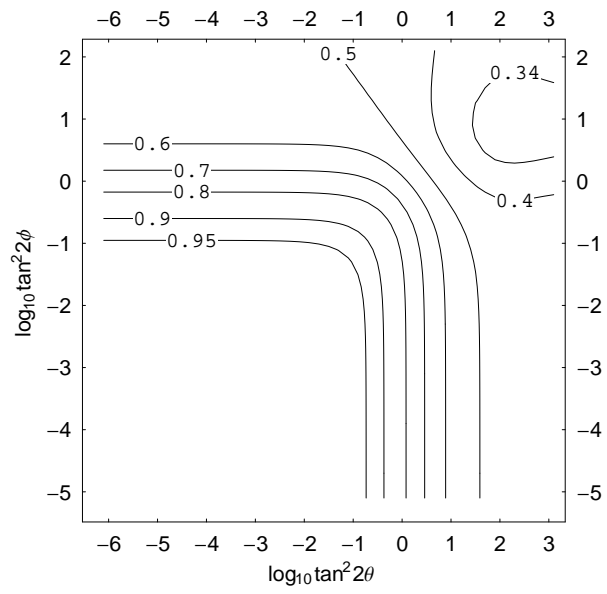


FIG. 2

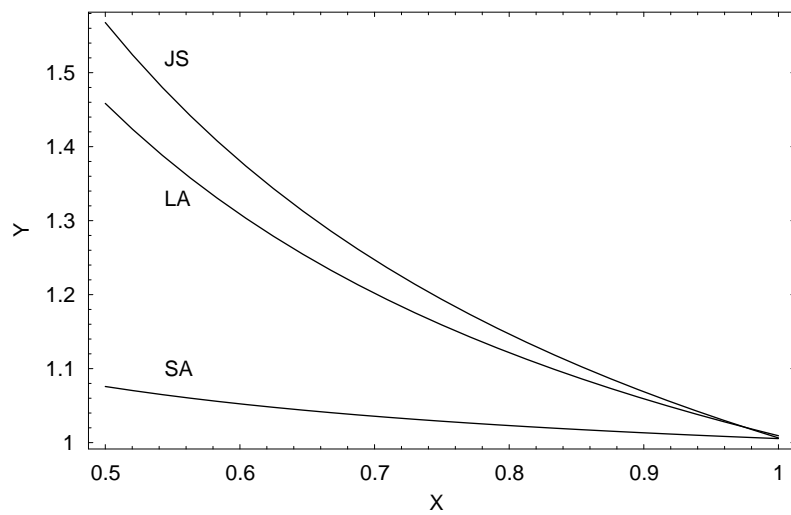


FIG. 3

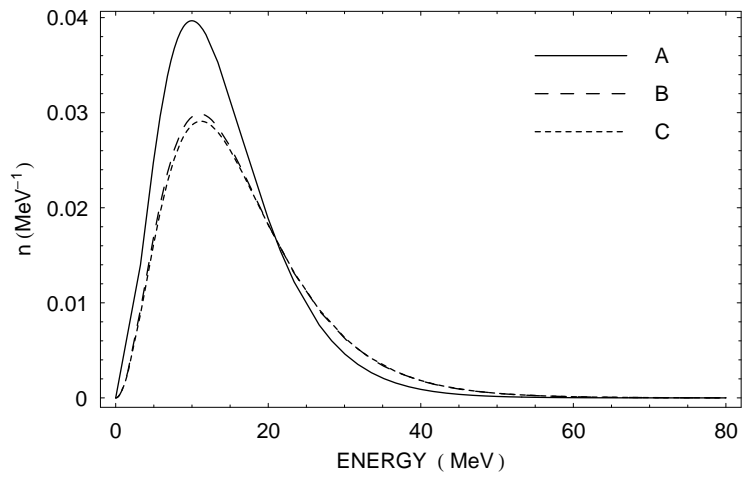


FIG. 4

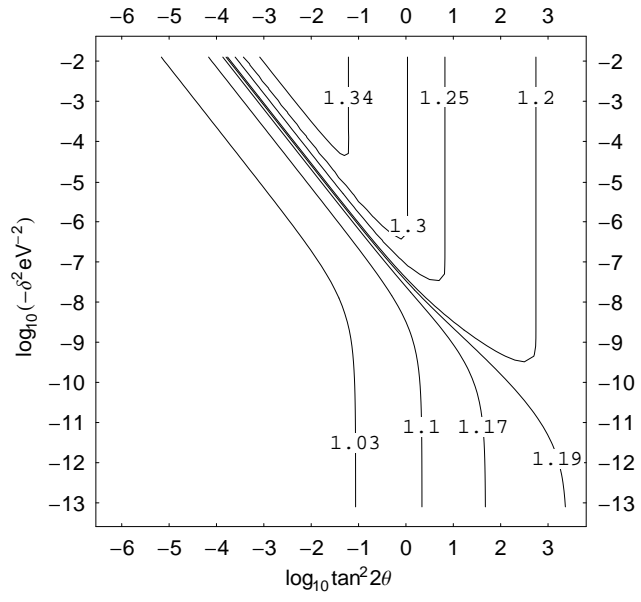


FIG. 5

